

# Thermodynamic Stability and the Origins of Incongruent and Strongly Coupled Diffusion in Solutions of Micelles, Solubilizates, and Microemulsions<sup>†</sup>

Jonathan R. Moulins, Jennifer A. MacNeil, and Derek G. Leaist\*

Department of Chemistry, St. Francis Xavier University, Antigonish, Nova Scotia, Canada B2G 2W5

Ternary mutual diffusion coefficients ( $D_{ik}$ ) are reported for aqueous solutions of dodecylsulfobetaine (1) + hexadecylsulfobetaine (2) mixed zwitterionic micelles. Cross-coefficient  $D_{12}$  reaches values almost as large as the main  $D_{ii}$  coefficients, indicating strongly coupled fluxes. As the surfactant concentrations are raised and the extent of micelle formation increases, values of the determinant  $D_{11}D_{22} - D_{12}D_{21}$  of the  $D_{ik}$  matrix drop sharply. Previous studies have shown that the thermodynamic stability constraint  $\mu_{11}\mu_{22} - \mu_{12}\mu_{21} \geq 0$  on the concentration derivatives  $\mu_{ik} = \partial\mu_i/\partial C_k$  of the chemical potentials causes  $D_{11}D_{22} - D_{12}D_{21}$  to vanish at critical points and phase separation boundaries. Consequently, the cross-coefficients become similar in magnitude to the main coefficients. Prompted by the insight that might be gained by demonstrating an analogy between diffusion in micelle solutions and diffusion near phase separation, a model of mixed-micelle formation based on multiple monomer association equilibria [ $nA_1 + mB_1 = A_nB_m$ ] is used to show that  $\mu_{11}\mu_{22} - \mu_{12}\mu_{21}$  drops almost to zero with increasing extent of micelle formation. This result, which is generalized to other association colloids, points to thermodynamics as the underlying cause of strongly coupled fluxes, incongruent diffusion, and other remarkable features of diffusion in solutions of mixed micelles, solubilizates, and microemulsions. A molecular interpretation of diffusion in these systems, consistent with the Gibbs–Duhem and Onsager reciprocal relations, is developed by relating the  $D_{ik}$  coefficients and the Onsager  $L_{ik}$  transport coefficients to the concentrations and the mobilities of the free monomers and various  $A_nB_m$  species.

## Introduction

Solutions of micelles,<sup>1–4</sup> solubilizates,<sup>5,6</sup> and microemulsions<sup>7–9</sup> demonstrate intriguing diffusion behavior. Mutual diffusion fluxes in these systems

$$J_i = - \sum_{k=1}^{n-1} D_{ik} \nabla C_k \quad (1)$$

can be very strongly coupled, as indicated by cross-diffusion coefficients  $D_{ik}$  ( $i \neq k$ ) that are routinely larger than the main  $D_{ii}$  coefficients. More remarkably, incongruent diffusion has been reported for ternary solutions ( $n = 3$ ) of mixed surfactant micelles.<sup>2</sup> One of the main  $D_{ii}$  diffusion coefficients is negative for these solutions. This means that a surfactant can diffuse “up” its own concentration gradient, from lower to higher concentrations. Mutual diffusion in microemulsions is counterintuitive and peculiar.<sup>7</sup> In water-in-oil microemulsions, for example, the water (1) and surfactant (2) components diffuse together through the oil-continuous solvent as surfactant-coated microdroplets of water. Yet the surfactant diffuses more rapidly than water ( $D_{22} > D_{11}$ ); the diffusion of water drives counter-current coupled flows of surfactant ( $D_{21} < 0$ ); and the diffusion of surfactant drives cocurrent coupled flows of water ( $D_{12} > 0$ ).<sup>7–9</sup> Diffusion data for association colloids are widely used to evaluate particle sizes and aggregation numbers and to predict rates of solubilization, emulsification, nucleation, and carrier-mediated transport.

The equally remarkable diffusion properties of solutions near critical points and phase separation boundaries have been studied

more extensively.<sup>10–22</sup> At compositions approaching phase separation, the cross-diffusion coefficients become similar in magnitude to the main coefficients. In addition, incongruent diffusion is observed.<sup>18–20</sup> Fick equations (eq 1) provide a useful description of this behavior in terms of conveniently measurable concentration gradients. For a better understanding of the unusual diffusion properties of solutions approaching instability, Onsager equations<sup>22–24</sup> prove to be helpful by relating the fluxes of the solution components to the gradients in chemical potentials, the fundamental driving forces for diffusion. The symmetrical Onsager transport coefficients ( $L_{ik} = L_{ki}$ ) describing the  $n - 1$  independent diffusion fluxes relative to solvent component  $n$

$$J'_i = - \sum_{k=1}^{n-1} L_{ik} \nabla \mu_k \quad (2)$$

are related to the mutual diffusion coefficients measured in volume-fixed laboratory coordinates by<sup>23,24</sup>

$$D_{ik} = \sum_{q=1}^{n-1} \sum_{m=1}^{n-1} L_{iq} \left( \delta_{qm} + \frac{C_q V_m}{C_n V_n} \right) \mu_{mk} \quad (3)$$

$\delta_{qm}$  is Kronecker's delta;  $V_m$  is the partial molar volume of component  $m$ ; and  $\mu_{mk}$  is the concentration derivative of the chemical potential of solute  $m$ .

$$\mu_{mk} = \left( \frac{\partial \mu_m}{\partial C_k} \right)_{T,p,c_{q \neq k}} \quad (4)$$

Minimization of the Gibbs free energy for thermodynamic equilibrium at fixed temperature and pressure requires<sup>18,20</sup>

\* Corresponding author. Tel.: (902) 867-5372. Fax: (902) 867-2414. E-mail: dleaist@stfx.ca.

<sup>†</sup> Part of the “William A. Wakeham Festschrift”.

$$\delta G_{T,p} = \sum_{k=1}^n \mu_{kk} \delta n_k = 0 \quad (5)$$

$$\delta^2 G_{T,p} = \sum_{m=1}^n \sum_{k=1}^n \mu_{mk} \delta n_m \delta n_k > 0 \quad (6)$$

To ensure positive values of  $\delta^2 G_{T,p}$  for arbitrary variations  $\delta n_m$ ,  $\delta n_k$  in the mole numbers, the  $\mu_{mm} \delta n_m^2$  terms in eq 6 must be positive, and therefore  $\mu_{mm} > 0$ . The theory of quadratic forms can also be used to show, less obviously, that the determinant of the  $\boldsymbol{\mu}$  matrix and its diagonal cofactors are positive for stable solutions.<sup>18,20</sup> Interestingly, thermodynamics imposes similar constraints on the  $L_{ik}$  transport coefficients.<sup>17,18,24</sup> Applying quadratic theory to the expression

$$T\sigma = - \sum_{i=1}^{n-1} J'_i \nabla \mu_i = \sum_{i=1}^{n-1} \sum_{k=1}^{n-1} L_{ik} \nabla \mu_i \nabla \mu_k > 0 \quad (7)$$

for the dissipation of free energy by diffusion indicates that the diagonal elements of  $\mathbf{L}$  are positive ( $L_{ii} > 0$ ), which means that a component cannot diffuse up its own chemical potential gradient. The determinant of  $\mathbf{L}$  and its diagonal cofactors are also positive.

$\mathbf{L}$  and  $\boldsymbol{\mu}$  are positive definite according to eqs 6 and 7. This information together with eq 3 can be used to prove that the eigenvalues  $D^{(i)}$  of the mutual diffusion coefficient matrix are real and positive for stable solutions:  $D^{(i)} > 0$ .<sup>14,17</sup> From the rules of matrix algebra, it follows that the trace and the determinant of  $\mathbf{D}$  are real and positive.

$$\text{tr } \mathbf{D} = \sum_{i=1}^{n-1} D_{ii} = \sum_{i=1}^{n-1} D^{(i)} > 0 \quad (8)$$

$$\det \mathbf{D} = \prod_{i=1}^{n-1} D^{(i)} > 0 \quad (9)$$

Thermodynamic stability criteria and the consequences for diffusion have been examined in detail.<sup>12–14,17,18</sup> For binary solutions of component 1 and solvent component 2, the stability constraints reduce to  $\mu_{11} \geq 0$  and  $D_{11} \geq 0$ , where  $D_{11}$  is the binary mutual diffusion coefficient ( $D$  in the usual notation). The equalities  $\mu_{11} = 0$  and  $D_{11} = 0$  hold at critical solution points and at compositions along the spinodal curve marking the boundary between stable and unstable states with respect to phase separation. Clark and Rowley<sup>21</sup> accurately located the spinodal curve for methanol + *n*-hexane mixtures by extrapolating binary mutual diffusion coefficients measured at different compositions to zero.

Stability considerations for ternary diffusion in solutions of components 1 and 2 and solvent component 3 provide<sup>17–20</sup>

$$\mu_{11} \geq 0 \quad \mu_{22} \geq 0 \quad (10)$$

$$\mu_{11}\mu_{22} - \mu_{12}\mu_{21} \geq 0 \quad (11)$$

$$D^{(1)} \geq 0 \quad D^{(2)} \geq 0 \quad (12)$$

$$D_{11} + D_{22} \geq 0 \quad (13)$$

$$D_{11}D_{22} - D_{12}D_{21} \geq 0 \quad (14)$$

In addition, the following restrictions apply to the Onsager coefficients

$$L_{11} \geq 0 \quad L_{22} \geq 0 \quad (15)$$

$$L_{11}L_{22} - L_{12}L_{21} \geq 0 \quad (16)$$

$L_{11}$ ,  $L_{22}$ , and  $L_{11}L_{22} - L_{12}L_{21}$  are not required to vanish at critical points and phase separation boundaries as a consequence of eq 3,  $\det \boldsymbol{\mu} = 0$  and  $\det \mathbf{D} = 0$ .<sup>18</sup>

At compositions approaching instability, where  $D_{11}D_{22}$  and  $D_{12}D_{21}$  become almost identical, the cross-coefficients are similar in magnitude to the main coefficients, and hence diffusion is strongly coupled. Although the sum  $D_{11} + D_{22}$  is positive for stable solutions, one of the main coefficients can be negative in cases of incongruent diffusion.<sup>18–20</sup> The stability constraints on the  $D_{ik}$  coefficients given by eqs 13 and 14 have been verified by ternary diffusion measurements made near the critical solution points of water + cyclohexane + chloroform<sup>18,19</sup> and water + 2-propanol + cyclohexane<sup>20</sup> mixtures.

The work reported here is a study of ternary mutual diffusion in aqueous solutions of dodecyl sulfobetaine (SB12) + hexadecyl sulfobetaine (SB16) mixed zwitterionic micelles. The critical micelle concentration (cmc) of aqueous SB16 is quite low, 0.000 028 mol·dm<sup>-3</sup> at 25 °C.<sup>25</sup> SB12 and SB16 are therefore more strongly associated than the SB10, SB12, and SB14 surfactants used in a previous study of mixed-micelle diffusion.<sup>1</sup> As the concentrations of SB12 and SB16 are raised and the extent of micelle formation increases, we noticed a sharp drop in the values of  $D_{11}D_{22} - D_{12}D_{21}$ . Micelles are not true phases in the spirit of the Gibbs phase rule. Nevertheless, it is known from previous work that micelle formation in binary surfactant solutions sharply reduces  $\mu_{11}$ , which in turn causes a sharp drop in the binary mutual diffusion coefficient in the cmc region.<sup>26</sup> In this paper, the corresponding behavior is investigated for ternary surfactant solutions. Prompted by the insight that might be gained by establishing an analogy between mixed-micelle diffusion and coupled diffusion near phase separation boundaries, we use the chemical equilibrium model for micelle formation to estimate the concentration derivatives of the chemical potentials of mixed surfactants. The values of  $\mu_{11}\mu_{22} - \mu_{12}\mu_{21}$  for SB12 (1) + SB16 (2) solutions are found to decrease sharply with increasing extent of micelle formation, closely resembling the behavior of solutions approaching instability. This result, which we generalize to other important association colloids, points to thermodynamics as the underlying cause of strongly coupled fluxes, incongruent diffusion, and other interesting features of multicomponent mutual diffusion in solutions of micelles,<sup>1–4</sup> solubilizes,<sup>5,6</sup> and microemulsions.<sup>7–9</sup>

## Experimental Section

Ternary mutual diffusion coefficients of aqueous dodecyl sulfobetaine (1) + hexadecyl sulfobetaine (1) solutions were measured by the Taylor dispersion method.<sup>23</sup> The solutions were prepared by dissolving weighed amounts of the sulfobetaines (Sigma, 99 % purity) in distilled, deionized water in volumetric flasks. A metering pump maintained a steady flow of carrier solution through a Teflon dispersion tube (length 3000 cm, inner radius  $r = 0.0383_2$  cm). Samples of solution were introduced at the tube inlet using an injection valve fitted with a 0.020 cm<sup>3</sup> loop. Flow rates were adjusted to give retention times ( $t_R$ ) of about  $1.5 \cdot 10^4$  s. A differential refractometer HPLC detector (Agilent model 1100) monitored the broadened distribution of the dispersed samples at the tube outlet. The detector voltage  $V(t)$  was measured at timed intervals using a digital voltmeter.

**Binary Diffusion Measurements.** Diffusion coefficients for binary aqueous solutions of SB10, SB12, and SB14 have been reported previously,<sup>1,27</sup> but no diffusion data appear to be available for aqueous SB16 solutions. To help characterize the surfactant, a few diffusion measurements were made on binary aqueous SB16 solutions. In these experiments, SB16 solutions

at concentration  $C + \Delta C$  were injected into carrier solutions of composition  $C$ . Binary diffusion coefficients were evaluated by fitting the equation<sup>23,28</sup>

$$V(t) = V_0 + V_1 t + \Delta V_{\max} \sqrt{\frac{t_R}{t}} \exp\left(-\frac{12D(t-t_R)^2}{r^2 t}\right) \quad (17)$$

to the measured detector voltages, treating  $D$  as an adjustable least-squares parameter together with the retention time  $t_R$ , peak height  $\Delta V_{\max}$ , baseline voltage  $V_0$ , and the baseline slope  $V_1$  (included to allow for small linear drifts in the detector signal).

**Ternary Diffusion Measurements.** Dispersion profiles for the SB12 (1) + SB16 (2) solutions were generated by introducing samples of solution of composition  $C_1 + \Delta C_1$  and  $C_2 + \Delta C_2$  into carrier solutions of composition  $C_1, C_2$ . Ternary dispersion profiles are cumbersome functions of the  $D_{ik}$  coefficients. To simplify the analysis, it is convenient to use the expression for the detector signal<sup>29</sup>

$$V(t) = V_0 + V_1 t + \Delta V_{\max} \sqrt{\frac{t_R}{t}} \left[ W_1 \exp\left(-\frac{12D^{(1)}(t-t_R)^2}{r^2 t}\right) + W_2 \exp\left(-\frac{12D^{(2)}(t-t_R)^2}{r^2 t}\right) \right] \quad (18)$$

in terms of the eigenvalues of the  $D_{ik}$  matrix

$$D^{(1)} = \frac{D_{11} + D_{22} + (D_{11} - D_{22})\sqrt{1 + [4D_{12}D_{21}/(D_{11} - D_{22})^2]}}{2} \quad (19)$$

$$D^{(2)} = \frac{D_{11} + D_{22} - (D_{11} - D_{22})\sqrt{1 + [4D_{12}D_{21}/(D_{11} - D_{22})^2]}}{2} \quad (20)$$

and the normalized weighting factors

$$W_1 = \frac{(a + b\alpha_1)\sqrt{D^{(1)}}}{(a + b\alpha_1)\sqrt{D^{(1)}} + (1 - a - b\alpha_1)\sqrt{D^{(2)}}} \quad (21)$$

$$W_2 = 1 - W_1 \quad (22)$$

defined in terms of the  $a$  and  $b$  parameters

$$a = \frac{D_{11} - D^{(1)} - (R_1/R_2)D_{12}}{D^{(2)} - D^{(1)}} \quad (23)$$

$$b = \frac{D_{22} - D_{11} + (R_2/R_1)D_{21} - (R_1/R_2)D_{12}}{D^{(2)} - D^{(1)}} \quad (24)$$

and the ratio of the detector sensitivity to SB12 (1) and SB14 (2).

$$\frac{R_2}{R_1} = \frac{\partial V/\partial C_2}{\partial V/\partial C_1} \quad (25)$$

$\alpha_1$  is the fraction of the initial refractive index change contributed by SB12 (1).

$$\alpha_1 = \frac{R_1 \Delta C_1}{R_1 \Delta C_1 + R_2 \Delta C_2} \quad (26)$$

A nonlinear least-squares procedure was used to fit eq 18 to dispersion profiles measured for two or more different values of  $\alpha_1$  for each carrier stream. The adjustable least-squares parameters included  $a, b, D^{(1)}, D^{(2)}$ , and, for each profile, the

**Table 1. Binary Mutual Diffusion Coefficients of Aqueous SB16 Solutions at 25 °C**

$C$ ( $10^{-3} \text{ mol} \cdot \text{dm}^{-3}$ )	$D$ ( $10^{-5} \text{ cm}^2 \cdot \text{s}^{-1}$ )	$C$ ( $10^{-3} \text{ mol} \cdot \text{dm}^{-3}$ )	$D$ ( $10^{-5} \text{ cm}^2 \cdot \text{s}^{-1}$ )
1.00	0.0920	10.00	0.0878
1.00	0.0911	10.00	0.0873
2.00	0.0882	20.00	0.0867
2.00	0.0892	20.00	0.0863

**Table 2. Critical Micelle Concentrations, Aggregation Numbers, Micelle Diffusion Coefficients, and Monomer Diffusion Coefficients for Binary Aqueous Sulfobetaine Solutions<sup>1,25</sup> at 25 °C**

surfactant	cmc		$D_{\text{micelle}}$	$D_{\text{monomer}}$
	( $10^{-3} \text{ mol} \cdot \text{dm}^{-3}$ )	$n$	( $10^{-5} \text{ cm}^2 \cdot \text{s}^{-1}$ )	( $10^{-5} \text{ cm}^2 \cdot \text{s}^{-1}$ )
SB10	0.032	41	0.16	0.54
SB12	0.0027	56	0.11	0.50
SB14	0.00027	67	0.090	0.43
SB16	0.000028	71	0.088	(0.35) <sup>a</sup>

<sup>a</sup> Estimated by extrapolation of data for SB10, SB12, and SB14.

retention time  $t_R$ , peak height  $\Delta V_{\max}$ , baseline voltage  $V_0$ , and baseline slope  $V_1$ . The ternary mutual coefficients were calculated from the fitted parameters by using the expressions<sup>29</sup>

$$D_{11} = D_1 + \frac{a(1-a-b)}{b}(D^{(1)} - D^{(2)}) \quad (27)$$

$$D_{12} = \frac{R_2 a(1-a)}{R_1 b}(D^{(1)} - D^{(2)}) \quad (28)$$

$$D_{21} = \frac{R_1(a+b)(1-a-b)}{R_2 b}(D^{(2)} - D^{(1)}) \quad (29)$$

$$D_{22} = D_2 + \frac{a(1-a-b)}{b}(D^{(2)} - D^{(1)}) \quad (30)$$

The ratio  $R_2/R_1$  of the detector sensitivities was evaluated by taking the ratio of peak areas generated per mole of excess solute 1 and 2 injected into the carrier solutions. Small initial concentration differences ( $\leq 0.005 \text{ mol} \cdot \text{dm}^{-3}$ ) were used to ensure that the measured  $D_{ik}$  coefficients were independent of the initial concentration differences  $\Delta C_1, \Delta C_2$ .

## Results and Discussion

**Binary Diffusion Coefficients of Aqueous Sulfobetaine Solutions.** Binary mutual diffusion coefficients were measured for aqueous SB16 solutions at carrier-stream concentrations from  $0.001 \text{ mol} \cdot \text{dm}^{-3}$  to  $0.020 \text{ mol} \cdot \text{dm}^{-3}$ . Table 1 gives the results. Although dilute solutions were used, all of the measurements were made at concentrations well above the cmc of aqueous SB16, so the reported  $D$  values provide an estimate of the SB16 micelle diffusion coefficient:  $0.088 \cdot 10^{-5} \text{ cm}^2 \cdot \text{s}^{-1}$ . The very low cmc of the surfactant ruled out dispersion measurements for submicellar solutions for the determination of the SB16 free-monomer diffusion coefficient. Previously reported micelle and monomer diffusion coefficients, cmc values, and aggregation numbers for aqueous sulfobetaine surfactants<sup>1,25,27</sup> are summarized in Table 2.

Binary mutual diffusion coefficients for aqueous solutions of sulfobetaine surfactants, from SB10 to SB16, are plotted in Figure 1. With increasing alkyl chain length, the aggregation number increases. Also, the  $D$  values drop closer to zero as the surfactant concentration is raised through the cmc, illustrating the analogy with diffusion at phase separation boundaries, where  $D$  is zero.<sup>10,11,21</sup>

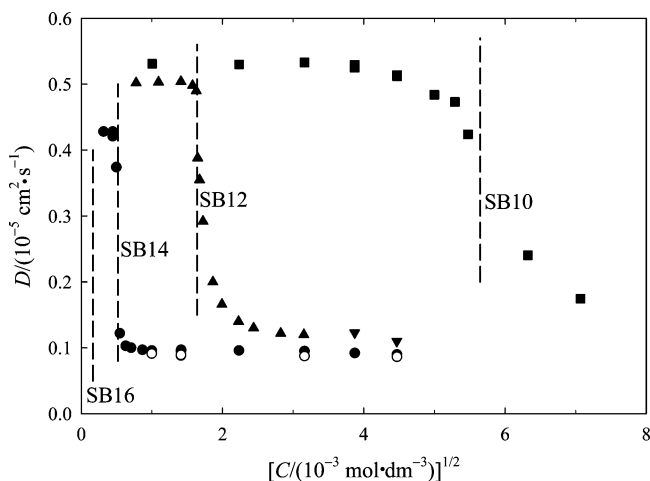


**Figure 1.** Binary mutual diffusion coefficients of aqueous  $\blacksquare$ , SB10;<sup>1</sup>  $\blacktriangle$ ,  $\blacktriangledown$ , SB12;<sup>1,27</sup>  $\bullet$ , SB14;<sup>1</sup> and  $\circ$ , SB16 (this work) solutions at 25 °C. The vertical dashed lines indicate the cmc for each surfactant. For clarity at the lower concentrations, the diffusion coefficients are plotted against the square root of the surfactant concentration.

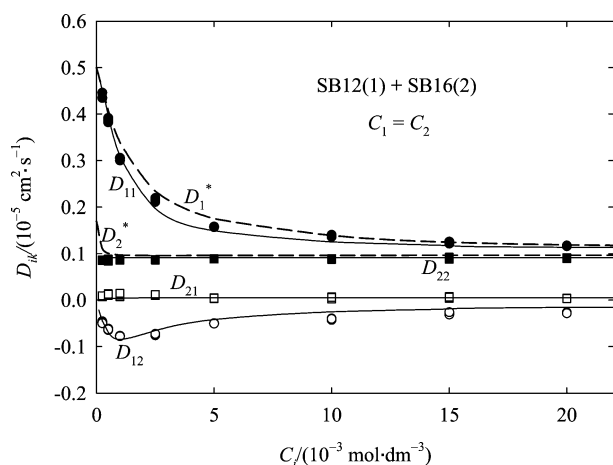


**Figure 2.** Diffusion coefficients of aqueous SB12 (1) + SB16 (2) solutions at 25 °C. Measured ternary mutual diffusion coefficients:  $\bullet$ ,  $\blacksquare$ ,  $\square$ ,  $\circ$ . Predicted ternary mutual diffusion coefficients: —, eqs 63 to 66. Average diffusion coefficients  $D_1^*$  and  $D_2^*$ : - - , eqs 60 and 61.

**Ternary Diffusion Coefficients of Aqueous SB12 (1) + SB16 (2) Solutions.** Ternary mutual diffusion coefficients were measured for aqueous SB12 (1) + SB16 (2) solutions containing equimolar amounts of surfactant ( $C_1 = C_2$ ) at total surfactant concentration from  $0.0005 \text{ mol} \cdot \text{dm}^{-3}$  to  $0.0400 \text{ mol} \cdot \text{dm}^{-3}$ . The  $D_{ik}$  coefficients evaluated from replicate sets of dispersion profiles at each composition were generally reproducible within  $\pm (0.005 \cdot 10^{-5} \text{ cm}^2 \cdot \text{s}^{-1})$ . The results are summarized in Table 3.

The composition dependence of the ternary diffusion coefficients is illustrated in Figure 2. The main coefficient  $D_{11}$  for SB12 is relatively large for the most dilute solutions ( $C_1 + C_2 < 0.002 \text{ mol} \cdot \text{dm}^{-3}$ ). At these dilutions, most of the SB12 diffuses as free monomers with diffusion coefficient<sup>1,27</sup>  $0.50 \cdot 10^{-5} \text{ cm}^2 \cdot \text{s}^{-1}$ . In the more concentrated solutions, where a larger proportion of the total SB12 component diffuses in micellar form,  $D_{11}$  is substantially lower. SB16, in contrast, diffuses almost entirely in micellar form in the solutions used in the present study, and  $D_{22}$  is consistently small ( $< 0.10 \cdot 10^{-5} \text{ cm}^2 \cdot \text{s}^{-1}$ ). Cross-coefficient  $D_{12}$  is negative and reaches the values almost as large as the main coefficients, which means that SB16 concentration gradients can drive substantial coupled

**Table 3.** Ternary Mutual Diffusion Coefficients Measured for Aqueous SB12 ( $C_1$ ) + SB16 ( $C_2$ ) Solutions at 25 °C

$C_1$	$C_2$	$D_{11}$	$D_{12}$	$D_{21}$	$D_{22}$	$D_{11}D_{22} - D_{12}D_{21}$
$10^{-3} \text{ mol} \cdot \text{dm}^{-3}$		$10^{-5} \text{ cm}^2 \cdot \text{s}^{-1}$				$10^{-5} \text{ cm}^4 \cdot \text{s}^{-2}$
0.25	0.25	0.435	-0.046	0.007	0.087	0.0377
0.25	0.25	0.434	-0.046	0.008	0.086	0.0376
0.25	0.25	0.435	-0.048	0.008	0.085	0.0374
0.25	0.25	0.446	-0.050	0.010	0.087	0.0391
0.50	0.50	0.386	-0.065	0.012	0.088	0.0344
0.50	0.50	0.391	-0.064	0.014	0.087	0.0345
0.50	0.50	0.382	-0.062	0.010	0.087	0.0338
0.50	0.50	0.387	-0.062	0.010	0.088	0.0339
0.50	0.50	0.385	-0.063	0.013	0.084	0.0328
1.00	1.00	0.306	-0.077	0.012	0.086	0.0314
1.00	1.00	0.305	-0.077	0.010	0.087	0.0314
1.00	1.00	0.306	-0.077	0.007	0.086	0.0314
1.00	1.00	0.305	-0.077	0.011	0.088	0.0319
1.00	1.00	0.300	-0.078	0.015	0.088	0.0316
2.50	2.50	0.218	-0.075	0.011	0.087	0.0215
2.50	2.50	0.211	-0.076	0.010	0.087	0.0217
2.50	2.50	0.218	-0.076	0.010	0.087	0.0216
2.50	2.50	0.217	-0.076	0.012	0.087	0.0215
2.50	2.50	0.218	-0.076	0.011	0.087	0.0216
2.50	2.50	0.219	-0.073	0.012	0.086	0.0214
5.00	5.00	0.157	-0.050	0.004	0.088	0.0158
5.00	5.00	0.157	-0.050	0.005	0.088	0.0159
5.00	5.00	0.158	-0.051	0.004	0.089	0.0160
5.00	5.00	0.158	-0.051	0.003	0.089	0.0160
5.00	5.00	0.157	-0.051	0.004	0.089	0.0159
10.00	10.00	0.137	-0.043	0.006	0.088	0.0124
10.00	10.00	0.136	-0.040	0.007	0.088	0.0122
10.00	10.00	0.140	-0.043	0.002	0.089	0.0126
10.00	10.00	0.138	-0.041	0.006	0.088	0.0123
15.00	15.00	0.126	-0.027	0.004	0.088	0.0112
15.00	15.00	0.124	-0.030	0.005	0.091	0.0114
15.00	15.00	0.125	-0.027	0.005	0.088	0.0111
15.00	15.00	0.125	-0.030	0.004	0.091	0.0115
15.00	15.00	0.121	-0.029	0.008	0.090	0.0112
15.00	15.00	0.123	-0.031	0.006	0.092	0.0116
15.00	15.00	0.124	-0.026	0.006	0.089	0.0111
20.00	20.00	0.116	-0.028	0.004	0.090	0.0106
20.00	20.00	0.116	-0.028	0.004	0.091	0.0107
20.00	20.00	0.117	-0.027	0.003	0.090	0.0106
20.00	20.00	0.116	-0.027	0.004	0.089	0.0105
20.00	20.00	0.117	-0.028	0.003	0.091	0.0107

fluxes of SB12, counter-current to the flux of SB16. The values of  $D_{21}$  are positive and relatively small.

Some difficulties were encountered in the least-squares analysis of the dispersion profiles. For the most concentrated solutions, unless accurate initial parameter estimates were used, the fitting procedure failed to converge and erroneously indicated complex values for the  $D^{(1)}$ ,  $D^{(2)}$  parameters. From stability considerations, eigenvalues  $D^{(1)}$  and  $D^{(2)}$  are real numbers.<sup>14,17,20</sup> This requirement, according to eqs 19 and 20, provides the constraint

$$(D_{11} - D_{22})^2 + 4D_{12}D_{21} \geq 0 \quad (31)$$

The source of the difficulty in the least-squares analysis of the dispersion profiles was revealed by examining the values of  $(D_{11} - D_{22})^2 + 4D_{12}D_{21}$ . With increasing surfactant concentration,  $(D_{11} - D_{22})^2 + 4D_{12}D_{21}$  plummets almost to zero, as shown in Figure 3. This result suggests that the eigenvalues of the  $D_{ik}$  matrix are closely approaching complex values that would indicate unstable solutions. During the curve-fitting calculations, inaccurate initial estimates of the  $D^{(1)}$ ,  $D^{(2)}$  fitting parameters produced unreliable iterations that led the parameter search into the nearby complex field. Values of the determinant  $\det \mathbf{D} = D_{11}D_{22} - D_{12}D_{21}$  are also plotted in Figure 3. The drop in  $\det \mathbf{D}$  with increasing surfactant concentration, though less dramatic,



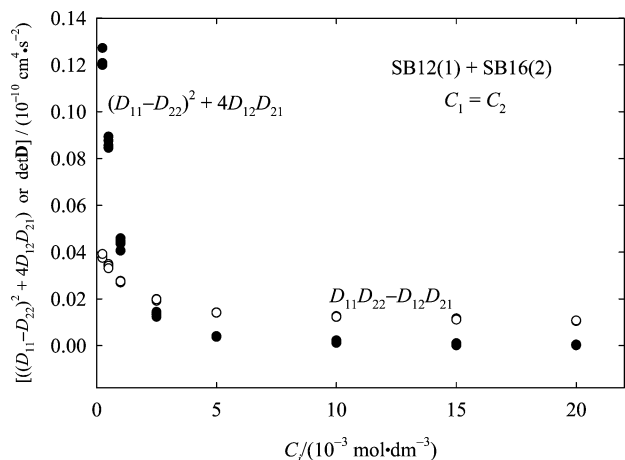


**Figure 3.** Values of  $(D_{11} - D_{22})^2 + 4D_{12}D_{21}$  and  $D_{11}D_{22} - D_{12}D_{21}$  for aqueous SB12 (1) + SB16 (2) solutions.

also suggests that stability considerations might be playing an important role in the diffusion behavior of the mixed surfactants.

#### Chemical Equilibrium Model for SB12 (1)–SB16 (2)

**Mixed-Micelle Formation.** Testing for a possible analogy between coupled diffusion in the mixed-micelle solutions and coupled diffusion in solutions near phase separation requires thermodynamic activity data for aqueous SB12 (1) and SB16 (2). The activities can be used to calculate the concentration derivatives of the surfactant chemical potentials to examine the behavior of  $\mu_{11}\mu_{22} - \mu_{12}\mu_{21}$  with increasing surfactant concentration. Because the surfactant solutions used in the present study are dilute and nonionic, they may be treated as ideal solutions of micelles and free surfactant monomers without serious error. With this simplification, the activities of the SB12 (1) and SB16 (2) components on the molarity scale are the concentrations of the free SB12 and SB16 monomers,<sup>30</sup> denoted here by  $c_{A1}$  and  $c_{B1}$ , respectively.

We will use the chemical equilibrium model of micelle formation, which is consistent with the Gibbs–Duhem relation,<sup>30</sup>  $\mu_{12} = \mu_{21}$ , to estimate the surfactant activities. Given values of the equilibrium constants  $K_{nm}$  for the formation of  $A_nB_m$  micelles by the association of  $n$  SB12 monomers and  $m$  SB16 monomers



the concentrations of the micelles and free surfactant monomers can be calculated by solving the equations for chemical equilibrium and mass balance

$$K_{nm} = \frac{c_{A_nB_m}}{c_{A1}^n c_{B1}^m} \quad (33)$$

$$C_1 = \sum_{n=1}^{\infty} \sum_{m=0}^{\infty} n c_{A_nB_m} = \sum_{n=1}^{\infty} \sum_{m=0}^{\infty} n K_{nm} c_{A1}^n c_{B1}^m \quad (34)$$

$$C_2 = \sum_{n=0}^{\infty} \sum_{m=1}^{\infty} m c_{A_nB_m} = \sum_{n=0}^{\infty} \sum_{m=1}^{\infty} m K_{nm} c_{A1}^n c_{B1}^m \quad (35)$$

SB12 and SB16 have identical sulfobetaine head groups and alkyl chains of similar length. Consequently, they form ideal mixed micelles with cmc values given by<sup>1,31,32</sup>

$$\text{cmc} = X_1 \text{cmc}_1 + (1 - X_1) \text{cmc}_2 = \left( \frac{f_1}{\text{cmc}_1} + \frac{1 - f_1}{\text{cmc}_2} \right)^{-1} \quad (36)$$

where  $\text{cmc}_1$  and  $\text{cmc}_2$  denote the cmc of binary aqueous SB12 (1) and SB16 (2) (Table 2);  $X_1$  is the mole fraction of SB12 in micelles

$$X_1 = n/(n + m) \quad (37)$$

and  $f_1$  is the solute fraction of the SB12 free monomers

$$f_1 = c_{A1}/(c_{A1} + c_{B1}) \quad (38)$$

The accurate approximation<sup>26</sup>  $K_{nm} = \text{cmc}^{1-n-m}$  together with eq 36 can be used to calculate the equilibrium constant for the formation of  $A_nB_m$  micelles.

$$K_{nm} = \frac{1}{f_1^n (1 - f_1)^m \text{cmc}^{n+m}} \quad (39)$$

To allow for a reasonable distribution of micelles, a set of equilibrium constants was adopted for the formation of micelles of composition  $X_1 = 0.00, 0.01, 0.02, \dots, 1.00$ . The logarithms of the equilibrium constants calculated in this manner are plotted in Figure 4. The corresponding aggregation numbers for the mixed micelles were calculated from the aggregation numbers of binary aqueous SB12 and SB16 solutions ( $n_0 = 56$  and  $m_0 = 71$ , respectively) and the linear relation

$$n + m = X_1 n_0 + (1 - X_1) m_0 \quad (40)$$

Equations 33 to 35 were solved numerically to calculate the free-monomer concentrations  $c_{A1}$ ,  $c_{B1}$  (the surfactant activities) at different total surfactant concentrations  $C_1$ ,  $C_2$ . The results are given in Table 4. A typical distribution of mixed micelles is illustrated in Figure 5 by plotting the fraction of micellar SB12 and SB16 as a function of micelle composition for a solution containing  $0.020 \text{ mol} \cdot \text{dm}^{-3}$  total surfactant. Equations 33 to 35 are a set of 101 coupled 71st-order polynomials in  $c_{A1}$  and  $c_{B1}$ . Solving these equations directly for  $c_{A1}$  and  $c_{B1}$  proved

**Table 4.** Free Monomer Concentrations (Surfactant Activities), Concentration Derivatives of the Surfactant Chemical Potentials, and Normalized  $\text{det}\mu$  Values for Aqueous SB12 ( $C_1$ ) + SB16 ( $C_2$ ) Solutions at 25 °C

$C_1$	$C_2$	$c_{A1}$	$c_{B1}$	$\mu_{11}/RT$	$\mu_{12}/RT = \mu_{21}/RT$	$\mu_{22}/RT$	$(\mu_{11}\mu_{22} - \mu_{12}\mu_{21})/(RT)^2$
$10^{-3} \text{ mol} \cdot \text{dm}^{-3}$				$\text{dm} \cdot \text{mol}^{-1}$			$\text{dm}^6 \cdot \text{mol}^{-2}$
0.00	0.00	0.0	0.0	$\infty$	0	$\infty$	$\infty$
0.10	0.10	0.0956	0.0215	10030.	-550.	221.	$2.34 \cdot 10^6$
0.25	0.25	0.221	0.0204	3968.	-488.	130.	$2.79 \cdot 10^4$
0.50	0.50	0.388	0.0188	1914.	-435.	136.	$7.14 \cdot 10^4$
1.00	1.00	0.605	0.0166	871.	-341.	155.	$1.85 \cdot 10^5$
2.50	2.50	0.860	0.0142	284.	-182.	127.	$2.87 \cdot 10^3$
5.00	5.00	0.980	0.0132	124.	-96.9	81.2	$6.84 \cdot 10^2$
10.00	10.00	1.05	0.0127	56.9	-49.4	45.7	$1.66 \cdot 10^2$
15.00	15.00	1.08	0.0126	36.8	-33.0	31.7	$7.28 \cdot 10^1$
20.00	20.00	1.10	0.0125	27.2	-24.8	24.2	$4.10 \cdot 10^1$
50.00	50.00	1.13	0.0125	10.5	-9.95	10.0	$6.34 \cdot 10^0$

to be vexatious. In practice, the calculation procedure was inverted by using estimates of  $c_{A1}$  and  $c_{B1}$  to calculate trial values of the total surfactant concentrations  $C_1$  and  $C_2$ . The latter were adjusted by Newton's method to give the desired total surfactant concentrations.

**Concentration Derivatives of the Chemical Potentials of SB12 (1) and SB16 (2).** Using the free-monomer concentrations  $c_{A1}$  and  $c_{B1}$  for the SB12 (1) and SB16 (2) activities gives

$$\mu_{11} = RT \left( \frac{\partial \ln c_{A1}}{\partial C_1} \right)_{T,p,C_2} \quad (41)$$

$$\mu_{12} = RT \left( \frac{\partial \ln c_{A1}}{\partial C_2} \right)_{T,p,C_1} \quad (42)$$

$$\mu_{21} = RT \left( \frac{\partial \ln c_{B1}}{\partial C_1} \right)_{T,p,C_1} \quad (43)$$

$$\mu_{22} = RT \left( \frac{\partial \ln c_{B1}}{\partial C_2} \right)_{T,p,C_1} \quad (44)$$

for the concentration derivatives of the surfactant chemical potentials. Differentiation of eqs 34 and 35 gives

$$dC_1 = Q_{11} d \ln c_{A1} + Q_{12} d \ln c_{B1} \quad (45)$$

$$dC_2 = Q_{21} d \ln c_{A1} + Q_{22} d \ln c_{B1} \quad (46)$$

with

$$Q_{11} = \sum_{n=1}^{\infty} \sum_{m=0}^{\infty} n^2 c_{AnBm} = \sum_{n=1}^{\infty} \sum_{m=0}^{\infty} n^2 K_{nm} c_{A1}^n c_{B1}^m \quad (47)$$

$$Q_{12} = Q_{21} = \sum_{n=1}^{\infty} \sum_{m=1}^{\infty} nmc_{AnBm} = \sum_{n=1}^{\infty} \sum_{m=1}^{\infty} nmK_{nm} c_{A1}^n c_{B1}^m \quad (48)$$

$$Q_{22} = \sum_{n=0}^{\infty} \sum_{m=1}^{\infty} m^2 c_{AnBm} = \sum_{n=1}^{\infty} \sum_{m=0}^{\infty} m^2 K_{nm} c_{A1}^n c_{B1}^m \quad (49)$$

which provides

$$\mu_{11} = \frac{RTQ_{22}}{Q_{11}Q_{22} - Q_{12}Q_{21}} \quad (50)$$

$$\mu_{12} = \mu_{21} = -\frac{RTQ_{12}}{Q_{11}Q_{22} - Q_{12}Q_{21}} \quad (51)$$

$$\mu_{22} = \frac{RTQ_{11}}{Q_{11}Q_{22} - Q_{12}Q_{21}} \quad (52)$$

Table 4 gives chemical potential derivatives calculated for SB12 (1) + SB16 (2) solutions at total surfactant concentrations up to  $0.040 \text{ mol} \cdot \text{dm}^{-3}$ . In very dilute solutions, below the cmc ( $0.000028 \text{ mol} \cdot \text{dm}^{-3}$  for equimolar SB12 + SB16 solutions), the surfactants diffuse entirely as free monomers. In this limiting case of no association ( $c_{A1} = C_1 = Q_{11}$ ,  $c_{B1} = C_2 = Q_{22}$ ,  $Q_{12} = Q_{21} = 0$ ),  $\mu_{12}$  and  $\mu_{21}$  are both zero and  $\mu_{11} = RT/C_1$  and  $\mu_{22} = RT/C_2$ . Above the cmc, association of the surfactant monomers reduces the values of  $\mu_{11}$  and  $\mu_{22}$  and produces negative values of  $\mu_{12}$  and  $\mu_{21}$ . Negative  $\mu_{12}$  and  $\mu_{21}$  derivatives can be understood by noting that added SB16 (2) increases the extent of micelle formation, thereby reducing the concentration of free SB12 (1) monomers and the SB12 (1) activity. Similarly, added SB16 (1) reduces the activity of SB16 (2).

Although negative values of  $\mu_{12}$  and  $\mu_{21}$  were anticipated, their magnitudes are surprisingly large. In fact,  $\mu_{12}$  and  $\mu_{21}$  are

only a few percent smaller than  $\mu_{11}$  and  $\mu_{22}$  at the highest surfactant concentrations. Consequently, the thermodynamic determinant  $\mu_{11}\mu_{22} - \mu_{12}\mu_{21}$  drops very sharply with increasing surfactant concentration (see Table 4). There is an inherent decrease in the  $\mu_{ik}$  values with increasing solute concentration, even for ideal solutions of nonassociating solutes, where  $\mu_{ii} = RT/C_i$ . To remove this bias, the values of  $\mu_{11}\mu_{22} - \mu_{12}\mu_{21}$  for the SB12 (1) + SB16 (2) solutions plotted in Figure 6 have been divided by  $\mu_{11}\mu_{22}$ .

$$\frac{\mu_{11}\mu_{22} - \mu_{12}\mu_{21}}{\mu_{11}\mu_{22}} = 1 - \frac{Q_{12}Q_{21}}{Q_{11}Q_{22}} \quad (53)$$

The values of  $\mu_{11}\mu_{22} - \mu_{12}\mu_{21}$ , normalized in this manner, drop from unity at infinite dilution to 0.06 at the highest surfactant concentration used in the calculations. The formation of micelles does not represent a true phase separation, so  $\mu_{11}\mu_{22} - \mu_{12}\mu_{21}$  does not drop to zero. Nevertheless, the behavior of the chemical potentials for the SB12 (1) + SB16 (2) solutions with increasing extent of micelle formation provides additional support for the analogy between coupled diffusion in mixed-micelle solutions and coupled diffusion in solutions approaching instability.

**Onsager  $L_{ik}$  Coefficients of Aqueous SB12 (1) + SB16 (2) Solutions.** The relatively large values of  $\mu_{12}$  and  $\mu_{21}$  indicate strong thermodynamic coupling of SB12 (1) and SB16 (2). It is interesting, therefore, to examine the  $L_{ik}$  transport coefficients describing the fluxes of the surfactants driven by chemical potential gradients, the thermodynamic driving forces for diffusion. The  $L_{ik}$  coefficients refer to solute fluxes relative to water, the solvent component. Partial molar volumes of the solution components are generally required to calculate the  $L_{ik}$  coefficients from the  $D_{ik}$  diffusion coefficients, which are measured in volume-fixed laboratory coordinates. Because dilute solutions were used in the present study, the distinction between the two reference frames is negligible and the  $L_{ik}$  coefficients can be calculated from the simpler relations

$$L_{11} = \frac{D_{11}\mu_{11} - D_{12}\mu_{21}}{\mu_{11}\mu_{22} - \mu_{12}\mu_{21}} \quad (54)$$

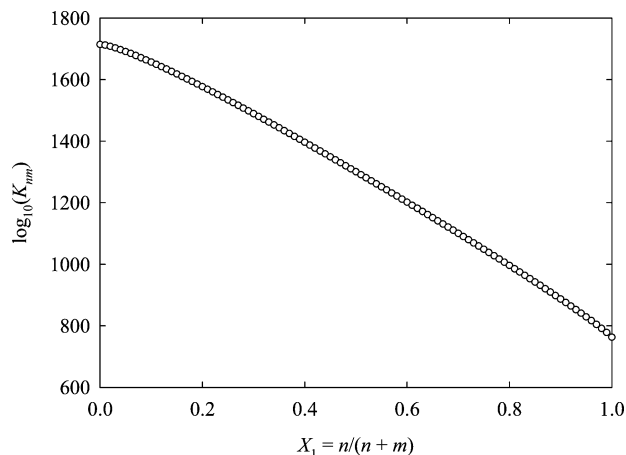
$$L_{12} = \frac{D_{11}\mu_{12} - D_{12}\mu_{22}}{\mu_{11}\mu_{22} - \mu_{12}\mu_{21}} \quad (55)$$

$$L_{21} = \frac{D_{21}\mu_{11} - D_{22}\mu_{21}}{\mu_{11}\mu_{22} - \mu_{12}\mu_{21}} \quad (56)$$

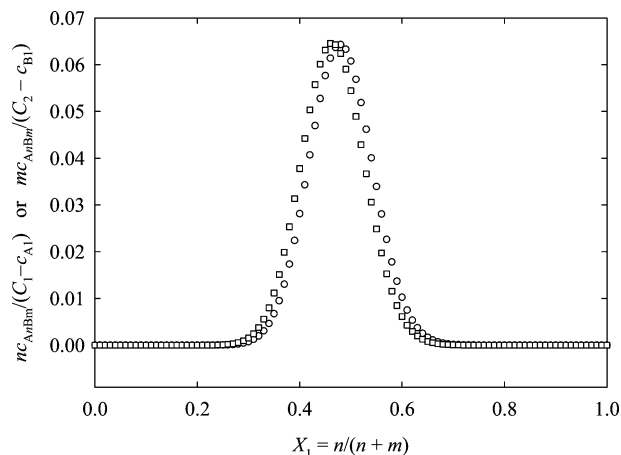
$$L_{22} = \frac{D_{21}\mu_{12} - D_{22}\mu_{22}}{\mu_{11}\mu_{22} - \mu_{12}\mu_{21}} \quad (57)$$

Table 5 gives the  $L_{ik}$  coefficients calculated for the SB12 (1) + SB16 (2) solutions. Cross-coefficients  $L_{12}$  and  $L_{21}$  are relatively large and exceed the value of main coefficient  $L_{11}$  at several compositions. Remarkably, all four  $L_{11}$ ,  $L_{12}$ ,  $L_{21}$ , and  $L_{22}$  coefficients approach nearly identical values at the highest surfactant concentrations. This behavior does not appear to have been reported previously. In contrast to the behavior of  $\det \mathbf{D}$  and  $\det \boldsymbol{\mu}$ , Table 5 shows that  $\det \mathbf{L}$  increases as the surfactant concentration is raised.

$L_{11}/C_1$  and  $L_{22}/C_2$  are the molar mobilities of the SB12 (1) and SB16 (2) components (the diffusion velocity developed per unit driving force). Values of  $RTL_{ik}/C_i$  are plotted in Figure 7. At the lowest concentrations, where most of the SB12 (1) component diffuses as free monomers, the mobility of the surfactant is relatively low because the transport of surfactant as separate monomers experiences more friction than the



**Figure 4.** Equilibrium constants for the micelle formation reactions  $nA_1 + mB_1 = A_nB_m$ .



**Figure 5.** Micellar distribution of  $\square$ , SB12 and  $\circ$ , SB16 for solutions containing  $0.010 \text{ mol} \cdot \text{dm}^{-3}$  SB12 +  $0.010 \text{ mol} \cdot \text{dm}^{-3}$  SB16.

transport of the equivalent number of monomers in a more compact micelle.<sup>26</sup>

The diffusion coefficient ratio  $D_{21}/D_{11}$  provides a convenient measure of the strength of the coupled diffusion of SB16 (2) in terms of Fick equations. It gives the number of moles of SB16 (2) transported per mole of SB12 (1) driven by its own concentration gradient. Similarly,  $D_{12}/D_{22}$  gives the number of

moles of SB12 (1) transported per mole of SB16 (2).  $D_{21}/D_{11}$  and  $D_{12}/D_{22}$  for the SB12 (1) + SB16 (2) solutions reach values as large as 0.05 and  $-0.89$ , respectively. The corresponding ratios  $L_{21}/L_{11}$  and  $L_{12}/L_{22}$  indicate the strength of coupled diffusion driven by chemical potential gradients.  $L_{21}/L_{11}$  and  $L_{12}/L_{22}$  for the SB12 (1) + SB16 (2) solutions reach values as large as 0.95 and 0.98, respectively. This comparison shows that the

**Table 5.** Onsager Coefficients of Aqueous SB12 ( $C_1$ ) + SB16 ( $C_2$ ) Solutions at 25 °C

$C_1$	$C_2$	$RTL_{11}$	$RTL_{12}$	$RTL_{21}$	$RTL_{22}$	$RT^2(L_{11}L_{22} - L_{12}L_{21})$
$10^{-3} \text{ mol} \cdot \text{dm}^{-3}$		$10^{-12} \text{ mol} \cdot \text{cm}^{-1} \cdot \text{s}^{-1}$				$10^{-24} \text{ mol} \cdot \text{cm}^{-2} \cdot \text{s}^{-2}$
0.25	0.25	1.23	1.06	1.53	12.3	13.5
0.25	0.25	1.22	1.05	1.54	12.3	13.5
0.25	0.25	1.19	0.78	1.52	12.2	13.4
0.25	0.25	1.21	0.69	1.56	12.5	14.0
0.50	0.50	3.42	6.18	5.58	24.3	48.5
0.50	0.50	3.55	6.64	5.55	24.1	48.8
0.50	0.50	3.54	6.78	5.52	24.0	47.6
0.50	0.50	3.55	6.83	5.53	24.1	47.8
0.50	0.50	3.48	6.47	5.35	23.2	46.3
1.00	1.00	11.4	20.2	16.9	42.8	148.
1.00	1.00	11.3	20.0	16.9	42.8	147.
1.00	1.00	11.4	20.1	16.6	42.1	146.
1.00	1.00	11.3	19.9	17.1	43.5	150.
1.00	1.00	10.8	18.7	17.4	44.0	148.
2.50	2.50	48.7	64.0	60.0	93.0	689.
2.50	2.50	45.1	58.8	59.6	92.5	666.
2.50	2.50	48.2	63.2	60.0	93.1	693.
2.50	2.50	47.8	62.7	60.5	93.7	689.
2.50	2.50	48.2	63.2	60.1	93.2	692.
2.50	2.50	50.6	66.9	59.6	92.4	687.
5.00	5.00	115.	131.	129.	165.	2050.
5.00	5.00	115.	131.	131.	167.	2060.
5.00	5.00	116.	132.	130.	166.	2080.
5.00	5.00	115.	132.	130.	166.	2080.
5.00	5.00	114.	130.	131.	167.	2070.
10.00	10.00	250.	260.	280.	321.	7440.
10.00	10.00	254.	266.	280.	321.	7320.
10.00	10.00	258.	269.	271.	312.	7570.
10.00	10.00	257.	269.	276.	317.	7380.
15.00	15.00	422.	432.	417.	463.	5400.
15.00	15.00	405.	413.	436.	484.	15700.
15.00	15.00	420.	430.	420.	467.	15200.
15.00	15.00	407.	416.	432.	479.	15800.
15.00	15.00	397.	406.	431.	491.	15400.
15.00	15.00	393.	401.	447.	496.	15900.
15.00	15.00	419.	429.	429.	476.	15300.
20.00	20.00	521.	523.	568.	620.	25900.
20.00	20.00	513.	514.	576.	629.	26000.
20.00	20.00	530.	532.	561.	612.	25800.
20.00	20.00	523.	525.	564.	616.	25600.
20.00	20.00	518.	520.	572.	624.	26200.

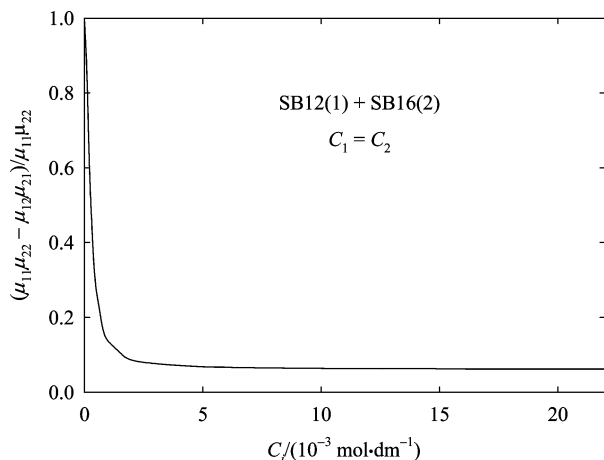


**Figure 6.** Normalized thermodynamic determinant (eq 53) plotted against surfactant concentration for equimolar SB12 ( $C_1$ ) + SB16 ( $C_2$ ) solutions.

surfactant fluxes driven by chemical potential gradients, the true driving forces for diffusion, are more strongly coupled than indicated by the Fick equations employed in most diffusion studies. Curiously,  $D_{12}$  is large and negative at several compositions, but  $L_{12}$  is large and positive.

Strongly coupled diffusion is prohibited in most solutions because the demixing caused by substantial coupled flows of components up their concentration gradient would increase the Gibbs free energy. At compositions near phase separation, in contrast, coupled diffusion can produce relatively large concentration gradients with little change in the free energy. This point can be illustrated by considering ternary diffusion at a fixed chemical potential of solute 2. From eq 7, the rate of dissipation of the Gibbs free energy is

$$(T\sigma)_{\mu_2} = L_{11}(\nabla\mu_1)_{\mu_2}^2 \quad (58)$$

By using  $d\mu_1 = \mu_{11}dC_1 + \mu_{12}dC_2$  and  $d\mu_2 = \mu_{21}dC_1 + \mu_{22}dC_2$ , eq 58 is equivalent to

$$\begin{aligned} (T\sigma)_{\mu_2} &= L_{11} \left( \mu_{11} - \frac{\mu_{12}\mu_{21}}{\mu_{22}} \right)^2 (\nabla C_1)_{\mu_2}^2 \\ &= L_{11} \left( \mu_{12} - \frac{\mu_{11}\mu_{22}}{\mu_{21}} \right)^2 (\nabla C_2)_{\mu_2}^2 \end{aligned} \quad (59)$$

At compositions approaching phase separation, where  $\mu_{11}\mu_{22} - \mu_{12}\mu_{21}$  becomes vanishingly small, coupled diffusion can produce large concentration gradients with little dissipation of free energy.

The Onsager coefficients for the SB12 (1) + SB16 (2) solutions (Table 5, Figure 7) show small deviations from the reciprocal relation  $L_{12} = L_{21}$ . The present study, however, was not undertaken to test the reciprocal relation for ternary diffusion. Such a test would require measured activities for the mixed surfactant solutions. The relatively small differences between  $L_{12}$  and  $L_{21}$  are consistent with experimental errors in the measured diffusion coefficients and with errors in the  $\mu_{ik}$  derivatives used in the calculations. The latter are difficult to estimate. Uncertainties in the cmc values used for the binary surfactant solutions could produce errors of several percent in the mixed surfactant activities and larger relative errors in the  $\mu_{ik}$  derivatives. The ensuing errors in the derived  $L_{ik}$  coefficients are magnified by the  $(\mu_{11}\mu_{22} - \mu_{12}\mu_{21})^{-1}$  factor in the  $\mathbf{L} = \mathbf{D}\boldsymbol{\mu}^{-1}$

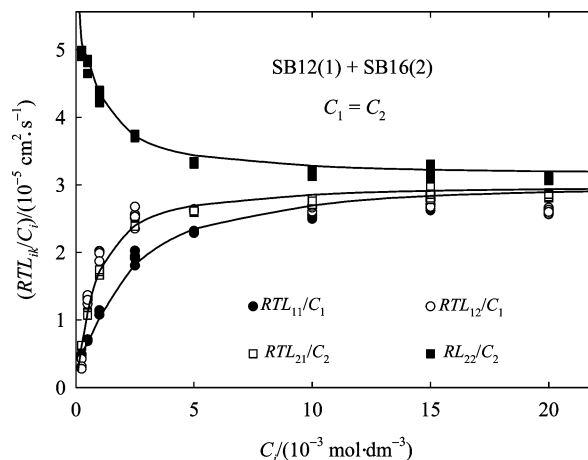


**Figure 7.**  $RTL_{ik}/C_i$  for SB12 ( $C_1$ ) + SB16 ( $C_2$ ) solutions. Measured values: ●, ○, ■, □. Predicted values: —.

calculations. The reliability of the reported  $L_{ik}$  coefficients is discussed in the next section.

**Predicted  $D_{ik}$  and  $L_{ik}$  Coefficients.** Mean diffusion coefficients for the SB12 (1) and SB16 (2) surfactant components can be evaluated by taking the simple concentration-weighted averages of the diffusion coefficients of the various SB12- and SB16-containing species ( $A_1$  and  $B_1$  free monomers and the  $A_nB_m$  micelles).

$$D_1^* = \frac{\sum_{n=1}^{\infty} \sum_{m=0}^{\infty} n c_{AnBm} D_{AnBm}}{C_1} \quad (60)$$

$$D_2^* = \frac{\sum_{n=0}^{\infty} \sum_{m=1}^{\infty} m c_{AnBm} D_{AnBm}}{C_2} \quad (61)$$

According to the Stokes–Einstein law, the micelle diffusion coefficients  $D_{AnBm}$  are inversely proportional to the cube root of the micelle volume,  $D_{AnBm} \propto (nV_1 + mV_2)^{-1/3}$ , which leads to the convenient expression

$$D_{AnBm} = \left[ \frac{n/n_0}{(D_{An0}^0)^3} + \frac{m/m_0}{(D_{Bm0}^0)^3} \right]^{-1/3} \quad (62)$$

for the mixed-micelle diffusion coefficients in terms of the pure-micelle diffusion coefficients  $D_{An0}$ ,  $D_{Bm0}$  and the aggregation numbers  $n_0$ ,  $m_0$  for binary aqueous solutions of the surfactants. The dashed curves plotted in Figure 2 give the mean diffusion coefficients calculated for SB12 (1) and SB16 (2) using the data in Table 2.

The average diffusion coefficients are related to the ternary mutual diffusion coefficients for the SB12 (1) + SB16 (2) solutions by<sup>9</sup>

$$D_{11} = \left[ \frac{\partial(C_1 D_1^*)}{\partial C_1} \right]_{C_2} \quad (63)$$

$$D_{12} = \left[ \frac{\partial(C_1 D_1^*)}{\partial C_2} \right]_{C_1} \quad (64)$$

$$D_{21} = \left[ \frac{\partial(C_2 D_2^*)}{\partial C_1} \right]_{C_2} \quad (65)$$



$$D_{22} = \left[ \frac{\partial(C_2 D_2^*)}{\partial C_2} \right]_{C_1} \quad (66)$$

The  $D_{ik}$  coefficients predicted by eqs 63 to 66 are plotted in Figure 2 (solid curves) for comparison with the measured diffusion coefficients. In view of the good agreement obtained, serious errors in the values of  $L_{ik}$  or  $\mu_{ik}$  implicit in the  $D_{ik}$  predictions would appear to be unlikely.

The large negative values for cross-coefficient  $D_{12}$  can be interpreted by noting that added SB16 (2), due to its very low cmc, increases the extent of micelle formation, thereby reducing the concentration of free SB12 monomers and the average SB12 (1) diffusion coefficient:  $[\partial(C_1 D_1^*)/\partial C_2]_{C_1} < 0$ . The negative  $D_{12}$  values in this case reflect the coupled flux of relatively mobile free SB12 monomers up the SB16 concentration gradient. On the other hand, added SB12 has little effect on the concentration of free SB16 monomers because essentially all of the SB16 exists in micellar form. Increasing the concentration of SB12 does, however, slightly reduce the size of the mixed micelles. The resulting increase in the rate of diffusion of micellar SB16 down the SB12 gradient is indicated by small, positive  $D_{21}$  values:  $[\partial(C_2 D_2^*)/\partial C_1]_{C_2} > 0$ . Coupled diffusion in solutions of mixed SB micelles is discussed in more detail in ref 1.

Employing eqs 54 to 57, the  $D_{ik}$  coefficients from eqs 63 to 66 were used to predict the corresponding  $L_{ik}$  coefficients. The values of  $RTL_{ik}/C_i$  obtained in this manner are plotted in Figure 7. Encouraging agreement is obtained, generally within the scatter of the measured values. The predicted  $L_{ik}$  coefficients can be obtained more directly by an extension<sup>1,9</sup> of eqs 63 to 66, which gives

$$L_{11} = \left[ \frac{\partial(C_1 D_1^*)}{\partial \mu_1} \right]_{\mu_2} \quad (67)$$

$$L_{12} = \left[ \frac{\partial(C_1 D_1^*)}{\partial \mu_2} \right]_{\mu_1} \quad (68)$$

$$L_{21} = \left[ \frac{\partial(C_2 D_2^*)}{\partial \mu_1} \right]_{\mu_2} \quad (69)$$

$$L_{22} = \left[ \frac{\partial(C_2 D_2^*)}{\partial \mu_2} \right]_{\mu_1} \quad (70)$$

To provide a molecular picture of the  $L_{ik}$  coefficients, eqs 60 and 61 for the average  $D_1^*$  and  $D_2^*$  diffusion coefficients can be substituted into eqs 67 to 70 together with  $d\mu_1 = RTd \ln c_{A1}$  and  $d\mu_2 = RTd \ln c_{B1}$  to obtain

$$L_{11} = \frac{\sum_{n=1}^{\infty} \sum_{m=0}^{\infty} n^2 c_{AnBm} D_{AnBm}}{RT} \quad (71)$$

$$L_{11} = L_{21} = \frac{\sum_{n=1}^{\infty} \sum_{m=0}^{\infty} n m c_{AnBm} D_{AnBm}}{RT} \quad (72)$$

$$L_{22} = \frac{\sum_{n=0}^{\infty} \sum_{m=1}^{\infty} m^2 c_{AnBm} D_{AnBm}}{RT} \quad (73)$$

These equations relate the transport coefficients of the total surfactant components to the concentrations and the mobilities

of the free monomers and the various associated species. Equation 72 shows that the treatment is consistent with the Onsager reciprocal relation  $L_{12} = L_{21}$  for ternary diffusion.

**Other Association Colloids.** In practical applications, diffusion measurements are used to characterize solutions of micelles, solubilizates, and microemulsions and to interpret rates of solubilization and emulsifications. The chemical equilibrium model developed for diffusion in SB12 (1) + SB16 (2) solutions can be applied to other nonionic mixed surfactants and extended to other association colloids, such as surfactant (1) + solubilizate (2) solutions, water (1) + surfactant (2) in water-in-oil microemulsions, and oil (1) + surfactant (2) in oil-in-water microemulsions. Molecular association in many of these systems is reliably approximated by the formation of monodisperse aggregates  $nA_1 + mB_1 = A_n B_m$  with average aggregation numbers  $n$  and  $m$ , which gives  $Q_{11} = c_{A1} + n^2 c_{AnBm}$ ,  $Q_{12} = Q_{21} = n m c_{AnBm}$ ,  $Q_{22} = c_{B1} + m^2 c_{AnBm}$ , and

$$\frac{\mu_{11}\mu_{22} - \mu_{12}\mu_{21}}{\mu_{11}\mu_{22}} = 1 - \frac{(n m c_{AnBm})^2}{(c_{A1} + n^2 c_{AnBm})(c_{B1} + m^2 c_{AnBm})} \quad (74)$$

for the normalized thermodynamic determinant. If association is extensive ( $c_{A1} \ll C_1$  and  $c_{B1} \ll C_2$ ), then

$$\frac{\mu_{11}\mu_{22} - \mu_{12}\mu_{21}}{\mu_{11}\mu_{22}} = \frac{c_{A1}}{n C_1} + \frac{c_{B1}}{m C_2} \cong 0 \quad (75)$$

and strongly coupled diffusion can be anticipated ( $D_{11}D_{22} - D_{12}D_{21} \cong 0$ ), especially in cases of large aggregation numbers.

The stability interpretation of coupled diffusion in solutions of association colloids is illustrated by water (1) + Aerosol OT (2) + *n*-heptane water-in-oil microemulsions. The diffusion coefficient determinant  $D_{11}D_{22} - D_{12}D_{21}$  for this system, calculated using data from ref 8, is plotted in Figure 8. As the Aerosol OT:water ratio ( $C_2/C_1$ ) decreases, less Aerosol OT surfactant is available to coat a given amount of water, so the  $(H_2O)_n(AOT)_m$  droplets grow larger in size. Simultaneously, the microemulsion becomes less stable, and the values of  $D_{11}D_{22} - D_{12}D_{21}$  drop nearly to zero, resembling the behavior of a solution approaching phase separation. Aggregation numbers  $n$  and  $m$  for the  $(H_2O)_n(AOT)_m$  microemulsion droplets increase from about 70 and 30 at  $C_2/C_1 = 0.50$  to about 6500 and 330 at  $C_2/C_1 = 0.05$ .<sup>8</sup>

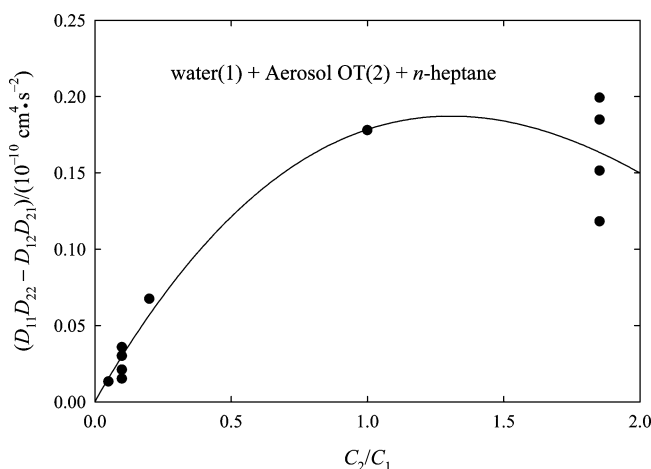


**Figure 8.** Determinant of the ternary mutual diffusion coefficient matrix for water (1) + Aerosol OT (2) water-in-oil microemulsions at 25 °C plotted against the Aerosol OT:water ratio.

## Conclusions

Ternary mutual diffusion measurements for aqueous solutions of SB12 (1) + SB16 (2) mixed zwitterionic micelles indicate that the eigenvalues of the  $D_{ik}$  matrix approach complex values and the determinant  $D_{11}D_{22} - D_{12}D_{21}$  drops sharply with the increasing extent of micelle formation. This behavior closely resembles the unusual diffusion properties of solutions approaching instability with respect to phase separation. At true phase separation boundaries, the thermodynamic stability constraint  $\mu_{11}\mu_{22} - \mu_{12}\mu_{21} = 0$  on the concentration derivatives of the chemical potentials causes  $D_{11}D_{22} - D_{12}D_{21}$  to vanish, and diffusion becomes strongly coupled. The analogy with coupled diffusion in SB12 (1) + SB16 (2) solutions is strengthened by using a multiple-association model of micelle formation to show that  $\mu_{11}\mu_{22} - \mu_{12}\mu_{21}$  drops to very low values with increasing extent of micelle formation. The model of mixed-micelle formation is sufficiently general to extend these ideas to microemulsions and other association colloids, suggesting that thermodynamics is the underlying cause of incongruent and strongly coupled diffusion in these systems. A molecular interpretation of coupled diffusion with multiple association equilibria, consistent with the Gibbs–Duhem and Onsager reciprocal relations, is developed by relating the chemical potential derivatives  $\mu_{ik}$ , the mutual diffusion coefficients  $D_{ik}$ , and Onsager transport coefficients  $L_{ik}$  to the concentrations and the mobilities of the free monomers and various associated species. In cases of extensive association, the results reported for aqueous SB12 (1) + SB16 (2) solutions illustrate that the strength of coupled diffusion measured by mutual diffusion coefficients and by Onsager coefficients can differ by orders of magnitude. Also,  $D_{ik}$  cross-coefficients and the corresponding  $L_{ik}$  cross-coefficient can have different signs, indicating that a gradient in the concentration of a solution component and the gradient in its chemical potential can drive large coupled flows in opposite directions.

## Literature Cited

- (1) Das, B.; Maitra, B.; Mercer, S. M.; Everist, M.; Leaist, D. G. A comparison of diffusion coefficients for ternary mixed micelle solutions measured by macroscopic gradient and dynamic light scattering techniques. *Phys. Chem. Chem. Phys.* **2008**, *10*, 3083–3092.
- (2) MacEwan, K.; Leaist, D. G. Incongruent diffusion (negative main diffusion coefficient) for a ternary mixed surfactant system. *J. Phys. Chem. B* **2002**, *106*, 10296–10300.
- (3) Leaist, D. G.; MacEwan, K. Coupled diffusion of mixed ionic micelles in sodium dodecyl sulfate + sodium octanoate solutions. *J. Phys. Chem. B* **2001**, *105*, 690–695.
- (4) MacEwan, K.; Leaist, D. G. Quaternary mutual diffusion coefficients for aqueous solutions of a cationic-anionic mixed surfactant from moments analysis of Taylor dispersion profiles. *Phys. Chem. Chem. Phys.* **2003**, *5*, 3951–3958.
- (5) Leaist, D. G.; Hao, L. A model for chemical interdiffusion of solubilizates and ionic micelles. *J. Chem. Soc., Faraday Trans.* **1995**, *91*, 2837–2842.
- (6) Leaist, D. G. Coupled diffusion of butanol solubilized in aqueous sodium dodecylsulfate micelles. *Can. J. Chem.* **1990**, *68*, 33–35.
- (7) Costantino, L.; Della Volpe, C.; Ortona, O.; Vitagliano, V. Isothermal diffusion in a peculiar ternary system: the microemulsion AOT-water-heptane. *J. Chem. Soc., Faraday Trans.* **1992**, *88*, 61–63.
- (8) Leaist, D. G.; Hao, L. Size distribution model for chemical interdiffusion in water/AOT/heptane water-in-oil microemulsions. *J. Phys. Chem.* **1995**, *99*, 12896–12901.
- (9) Leaist, D. G. Relating multicomponent mutual diffusion coefficients and intradiffusion coefficients for associating solutes. Application to coupled diffusion in water-in-oil microemulsions. *Phys. Chem. Chem. Phys.* **2002**, *4*, 4732–4739.
- (10) Claesson, S.; Sundelof, L.-O. Diffusion libre au voisinage de la temperature critique de miscibility. *J. Chim. Phys.* **1957**, *54*, 914–919.
- (11) Haase, R.; Siry, M. Diffusion im kritischen entmischungsbereich flussiger systeme. *Z. Phys. Chem. N. F.* **1968**, *57*, 56–73.
- (12) Kirkaldy, J. S. Diffusion in multicomponent metallic systems. I. Phenomenological theory for substitutional solid solution alloys. *Can. J. Phys.* **1958**, *36*, 899–906.
- (13) Kirkaldy, J. S.; Weichert, D.; Haq, Z. L. Diffusion in multicomponent metallic systems. VI. Some thermodynamic properties of the  $D$  matrix and the corresponding solutions of the diffusion equations. *Can. J. Phys.* **1963**, *41*, 2166–2173.
- (14) Kirkaldy, J. S.; Purdy, G. R. Diffusion in multicomponent metallic systems. X. Diffusion at and near ternary critical states. *Can. J. Phys.* **1969**, *47*, 865–871.
- (15) Sethy, A.; Cullinan, H. T. Transport of mass in ternary liquid-liquid systems. Part I. Diffusion studies. *AIChE J.* **1975**, *21*, 571–575.
- (16) Wakeham, W. A. Diffusion coefficient measurements by the chromatographic method. *Faraday Symp. Chem. Soc.* **1980**, *15*, 145–154.
- (17) Cullinan, H. T., Jr. Analysis of the flux equations of multicomponent diffusion. *Ind. Eng. Chem. Fundam.* **1965**, *4*, 133–139.
- (18) Vitagliano, V.; Sartorio, R.; Scala, S.; Spaduzzi, D. Diffusion in a ternary system and the critical mixing point. *J. Solution Chem.* **1978**, *7*, 605–621.
- (19) Buzatu, D.; Buzatu, F. D.; Paduano, L.; Sartorio, R. Diffusion coefficients for the ternary system water + chloroform + acetic acid at 25 °C. *J. Solution Chem.* **2007**, *36*, 1373–1384.
- (20) Clark, W. M.; Rowley, R. L. Ternary liquid diffusion coefficients near plait points. *Int. J. Thermophys.* **1985**, *6*, 631–642.
- (21) Clark, W. M.; Rowley, R. L. Ternary mutual diffusion coefficient of methanol - n-hexane near the consolute point. *AIChE J.* **1986**, *32*, 1125–1131.
- (22) Cussler, E. L., Jr. *Multicomponent Diffusion*; Elsevier: Amsterdam, 1976.
- (23) Tyrrell, H. J. V.; Harris, K. R. *Diffusion in Liquids*; Butterworths: London, 1984.
- (24) Haase, R. *Thermodynamics of Irreversible Processes*; Dover: New York, 1990.
- (25) Graciani, M. M.; Rodriguez, A.; Munoz, M.; Moya, M. L. Micellar solutions of sulfobetaine surfactants in water-ethylene glycol mixtures: surface tension, fluorescence, spectroscopic, conductimetric, and kinetic studies. *Langmuir* **2005**, *21*, 7161–7169.
- (26) Leaist, D. G. Binary diffusion of micellar electrolytes. *J. Colloid Interface Sci.* **1986**, *111*, 230–240.
- (27) Siderius, A.; Kolisnek-Kehl, S.; Leaist, D. G. Surfactant diffusion near critical micelle concentrations. *J. Solution Chem.* **2002**, *31*, 607–625.
- (28) Erkey, C.; Akgerman, A. In *Measurement of the Transport Properties of Fluids*; Wakeham, W. A., Nagashima, A., Sengers, J. V., Eds.; Blackwell: London, 1991.
- (29) Deng, Z.; Leaist, D. G. Ternary mutual diffusion coefficients of  $\text{MgCl}_2 + \text{MgSO}_4 + \text{H}_2\text{O}$  and  $\text{Na}_2\text{SO}_4 + \text{MgSO}_4 + \text{H}_2\text{O}$  from Taylor dispersion profiles. *Can. J. Chem.* **1991**, *69*, 1548–1553.
- (30) Acree, W. E., Jr. *Thermodynamic Properties of Nonelectrolyte Solutions*; Academic: New York, 1984.
- (31) Rosen, M. J. Synergism in mixtures of zwitterionic micelles. *Langmuir* **1991**, *7*, 885–888.
- (32) Schulz, P. C.; Rodriguez, J. L.; Minardi, R. M.; Sierra, M. B.; Morini, M. A. Are the mixtures of homologous surfactants ideal? *J. Colloid Interface Sci.* **2006**, *303*, 264–269.

Received for review October 16, 2008. Accepted November 28, 2008. Acknowledgement is made to the Natural Sciences and Engineering Research Council for the financial support of this research.

JE800767E